Long-range orientation correlation in water

David P. Shelton[a)]

Department of Physics and Astronomy, University of Nevada, Las Vegas, Nevada 89154-4002, USA

Strong short-range intermolecular interactions result in position and orientation correlations between nearest neighbour molecules in isotropic liquids, but it is generally assumed that such correlations extend at most a few molecular diameters. Results from second-harmonic light scattering experiments presented here reveal long-range molecular orientation correlations in liquid water, where the molecular dipole orientation distribution has the form of a nearly pure transverse vector field. Spatial scales in the range 200–2000 nm are probed by the angle-dependent measurements and the observed correlations are thought to result from rotation-translation coupling in acoustic phonons in the liquid. © 2014 AIP Publishing LLC. [http://dx.doi.org/10.1063/1.4903541]

It has long been understood that the shape of molecules and short-range steric effects exert the dominant influence on the local structure of liquids[1–3] and it is generally assumed that the intermolecular correlations in liquids extend at most a few molecular diameters. Liquids are intermediate between gases and crystalline solids but the structure of liquids is a more difficult problem. The intermolecular interactions are strong so they cannot be treated as small perturbations as in gases, and the molecular displacements are large so they cannot be treated as small perturbations of a fixed equilibrium structure as in solids. Experimentally, direct measurement of long-range structure in liquids by x-ray diffraction is defeated by the lack of positional order of the molecules. In contradiction to the usual assumption, recent experiments measuring second-harmonic or hyper-Rayleigh light scattering (HRS) have found evidence for long-range orientation correlations in several molecular liquids.[4] The present experiment was conducted to reveal the source of these correlations.

These experiments use HRS, which is mediated by the third-rank molecular hyperpolarizability β, to probe non-centrosymmetric fluctuations such as orientation fluctuations of polar molecules.[5,6] The present HRS measurements were made with linearly polarized light at scattering angles in the range from 0° to 180°, using apparatus and techniques similar to that previously described.[7,8] The scattering configurations with incident and scattered light polarized either perpendicular or parallel to the horizontal scattering plane are denoted VV, HV, VH, and HH, where V denotes vertical polarization, H denotes horizontal polarization, and the first and second letters refer to the incident and scattered light, respectively. The presence of polar collective modes and long-range molecular correlation is revealed in these experiments by the observation $I_{HV} \neq I_{VH}$ for the HRS intensities, which is forbidden by symmetry when only local correlations are present.

The HRS intensities at scattering angle θ in the horizontal plane, including contributions from randomly oriented molecules and from transverse and longitudinal polar collective modes, are given by the expressions[4,9,10]

$$I_{VV} = A_0 P^2 + A_T R^2, \tag{1}$$

$$I_{HV} = A_0 + A_T, \tag{2}$$

$$I_{VH} = A_0 + A_T \sin^2(\theta/2) + A_L \cos^2(\theta/2), \tag{3}$$

$$I_{HH} = A_0[\sin^2\theta + P^2\cos^2\theta]$$
$$+ A_T[1 - (R-1)\cos\theta]^2 \sin^2(\theta/2)$$
$$+ A_L[1 + (R-1)\cos\theta]^2 \cos^2(\theta/2). \tag{4}$$

The intensity coefficients for HRS from randomly oriented molecules, transverse, and longitudinal polar modes are A_0, A_T, and A_L, respectively. The polarization dependence for HRS from randomly oriented molecules is governed by the parameter P^2, which falls in the range $R^2 \geq P^2 \geq 3/2$, as determined by the relative size of the contributions from the first rank (vector) and third rank (octupolar) irreducible spherical tensor parts of β.[5] The HRS polarization dependence for polar modes is governed by the parameter R, which is determined by the vector part of β ($R = 3$ is obtained in the far-off-resonance limit where the Cartesian hyperpolarizability tensor has full permutation symmetry of spatial indices, i.e., Kleinman symmetry). The HRS signal observed in a particular direction is due to the Fourier components of the induced second-harmonic polarization vector field in the medium, with wavevector equal to the scattering wavevector $\mathbf{K} = 2\mathbf{k}_i - \mathbf{k}_s$, where $\mathbf{k}_i$ and $\mathbf{k}_s$ are the wavevectors of the incident and scattered photons, respectively. In these experiments the magnitude of the scattering wavevector is $K = K_{max}\sin(\theta/2)$, where $K_{max} \approx 8\pi n_\omega/\lambda_\omega = 2\pi/\Lambda_{min}$, the laser wavelength is $\lambda_\omega = 1064$ nm, and $\Lambda_{min} = 201$ nm for D_2O.

Table I shows HRS measurements made with 60 cm^{-1} spectral bandwidth for D_2O at $T = 25.0\,°C$. The HRS intensity ratios in Table I are extrapolated to zero collection aperture and corrected for ion contamination, as previously described.[7,8] The narrow spectral spike induced by dissolved ions rides on top of the much broader intrinsic HRS spectrum,[11] and it was measured by scanning the HRS

a)shelton@physics.unlv.edu

TABLE I. HRS intensity ratio measurements versus scattering angle for D_2O. The HRS intensities have been corrected for the ion-induced HRS contribution and 1 S.D. uncertainty in the last digit is shown in parentheses.

θ (deg)	$\dfrac{I_{VV}}{I_{HV}}$	$\dfrac{I_{HV}}{I_{VH}}$	$\dfrac{I_{HH}}{I_{VH}}$	$\dfrac{I_{VV}}{I_{VV}(90°)}$
0.0	7.0(3)	1.007(6)		0.54(2)
4.5	7.34(7)	3.55(11)	4.7(3)	
5.0	7.23(8)	4.12(9)	4.0(2)	
11.2	7.35(10)	4.30(8)	3.52(13)	
18.5	7.43(11)	3.99(10)	3.34(11)	
45.0	7.38(5)	2.97(3)	1.59(2)	0.99(2)
71.5	7.39(4)	2.053(15)	0.647(14)	
78.7	7.35(2)	1.864(17)	0.681(6)	
87.0[a]			0.884(4)	
90.0[a]	7.38(2)	1.631(4)	1.006(4)	
93.0[a]			1.152(4)	
108.5	7.39(4)	1.367(4)	2.169(8)	
135.0	7.39(2)	1.126(4)	4.66(2)	1.02(2)
180.0	7.32(2)	1.003(3)		0.87(10)

[a]From Ref. 4.

spectrum at 13 MHz resolution and then subtracted. Although a loop containing an ion-exchange resin column was used to de-ionize the sample (resistivity $\approx$ 50 MΩ cm), the residual ion-induced HRS contribution, which varies as $\tan^{-2}(\theta/2)$, was larger than the intrinsic HRS for some measurements at $\theta < 10°$. The sample cell was either a special 8-window cell for the 45°, 90°, and 135° measurements, or a standard square 10 mm fluorimeter cuvette. The Gaussian-mode laser beam was normally incident on the cell entrance window and focused to a 4.5 μm waist radius in the sample. Two-photon fluorescence from 0.1 mmol/l disodium fluorescein-D_2O solution was used for angle-dependent relative intensity calibration.

The scattering plane becomes undefined at forward scattering angle less than the focused laser beam divergence half-angle ($\theta_{1/2} = 3.3°$). The HRS contributions from Eqs. (1)–(4) are mixed as a result, giving the mixed HRS intensity ratios

$$\left(\frac{I_{VV}}{I_{HV}}\right)_{mix} = \frac{(1-g)I_{VV} + gI_{HH}}{(1-g)I_{HV} + gI_{VH}}, \quad (5)$$

$$\left(\frac{I_{HV}}{I_{VH}}\right)_{mix} = \frac{(1-g)I_{HV} + gI_{VH}}{(1-g)I_{VH} + gI_{HV}}, \quad (6)$$

$$\left(\frac{I_{HH}}{I_{VH}}\right)_{mix} = \frac{(1-g)I_{HH} + gI_{VV}}{(1-g)I_{VH} + gI_{HV}}, \quad (7)$$

where $g = (1/2)\exp(-x^2/x_0^2)$ and $x = \sin(\theta/2)$. Equations (1)–(7), which are fit to the data, contain five parameters: P^2, R, A_T/A_0, A_L/A_0, and x_0.

Figure 1 shows the HRS data and the fitted curves obtained using Eqs. (1)–(7) and setting $A_L = 0$. The incoherent HRS from randomly oriented molecules is described by the fit parameter P^2, while the transverse polar mode HRS contribution from orientationally correlated molecules is described by the fit parameters R and A_T/A_0. The best fit mixing parameter $x_0 = 0.026 \pm 0.001$ corresponds to 3.0° effective beam divergence in good agreement with $\theta_{1/2} = 3.3°$, and the mix-
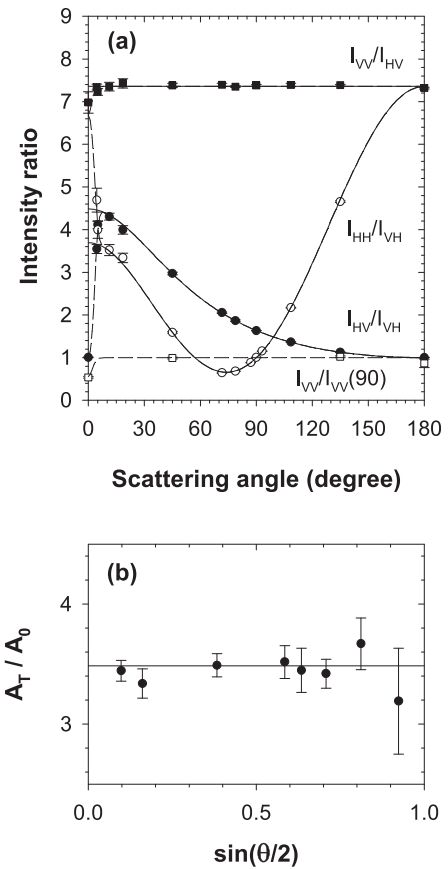
FIG. 1. HRS results for D_2O. (a) Scattering angle dependence of HRS intensity ratio measurements (symbols) and theoretical fit (curves) are compared. The dashed curves include (solid curves do not include) the effect of the focused laser beam divergence angle. Exactly the same fit curves are obtained with fit parameters $P^2 = 3.69 \pm 0.06$, $R = 2.900 \pm 0.005$, $A_T/A_0 = 3.49 \pm 0.04$, $A_L/A_0 = 0$, $x_0 = 0.026 \pm 0.001$, and with the alternative fit parameters $P^{*2} = 3/2$, $R = 2.900 \pm 0.005$, $A_T^*/A_0^* = 5.57 \pm 0.13$, $A_L^*/A_0^* = 0.46 \pm 0.02$, $x_0 = 0.026 \pm 0.001$. (b) Comparison of transverse mode strength A_T/A_0 determined from individual I_{HV}/I_{VH} measurements using Eq. (8) and $A_T/A_0 = 3.49$ (solid line) from the first fit in (a).

ing is negligible for $\theta > 10°$. The fitted value $R = 2.90$ is consistent with expected small deviations from Kleinman symmetry. The fit to the data is good and it shows that the transverse polar mode contribution dominates the HRS intensity. The possible K dependence of A_T/A_0 was investigated by inverting the expression for I_{HV}/I_{VH} as a function of A_T/A_0, obtained from Eqs. (2) and (3), to give

$$\frac{A_T}{A_0} = \frac{(I_{HV}/I_{VH}) - 1}{1 - (I_{HV}/I_{VH})\sin^2(\theta/2)}. \quad (8)$$

Values for A_T/A_0 versus $K/K_{max} = \sin(\theta/2)$ obtained directly from the I_{HV}/I_{VH} data using Eq. (8) are plotted in Fig. 1(b) and are consistent with A_T/A_0 independent of K, as is assumed for the fit shown in Fig. 1(a). The observed K range is $0.1 \leq K/K_{max} \leq 1$, corresponding to wavelength range 2000 nm $\geq \Lambda \geq$ 200 nm.

The fit parameters are not uniquely determined by the HRS intensity ratio data since the fitted curves obtained from Eqs. (1)–(7) are invariant for changes to alternative

parameters P'^2, A'_T/A'_0, A'_L/A'_0 where

$$\frac{P'^2 - R^2}{P^2 - R^2} = \frac{1 + A'_T/A'_0}{1 + A_T/A_0} = \frac{1 + A'_L/A'_0}{1 + A_L/A_0}. \quad (9)$$

The physical constraints, that A_0, A_T, A_L are all non-negative intensities, and $R^2 \geq P^2 \geq 3/2$, restrict the allowable range for the parameters. The maximum value for P^2 is obtained for $A_L = 0$, while the minimum value 3/2 for P^2 maximizes A_T and A_L. Exactly the same fit is obtained for all parameters sets satisfying the relations in Eq. (9). The choice of equivalent parameter sets arises since HRS from randomly oriented molecules can be expressed by different linear combinations of the A_0 term and the sum of polar mode terms with $A_T = A_L$ (which has exactly the same angular dependence as HRS from randomly oriented molecules). Information about orientation correlations is contained in the difference $A_T - A_L$.

The particular choice $P^{*2} = 3/2$ for P'^2 has special theoretical significance. The molecular hyperpolarizability tensor $\beta = \beta^{(1)} \oplus \beta^{(3)}$ is the direct sum of first- and third-rank irreducible spherical tensors, which contribute separately to the HRS intensity.[5] The octupolar irreducible third-rank part $\beta^{(3)}$ contributes to the A_0 mode with $I_{VV}/I_{HV} = 3/2$, and cannot contribute to polar modes, whereas the irreducible first-rank part $\beta^{(1)}$ transforms as a vector and can contribute to transverse and longitudinal polar collective modes. Since an arbitrary vector field representing the molecular orientation distribution can be expressed as the sum of longitudinal and transverse Fourier components, there is no loss of generality in the partition where the A_0 mode in Eqs. (1)–(4) is entirely due to $\beta^{(3)}$ and the A_T and A_L modes are due to $\beta^{(1)}$. The fit parameters with this partition are $P^{*2} = 3/2$, $R = 2.900 \pm 0.005$, $A^*_T/A^*_0 = 5.57 \pm 0.13$, $A^*_L/A^*_0 = 0.46 \pm 0.02$, and $x_0 = 0.026 \pm 0.001$. A random molecular orientation distribution would give $A^*_T = A^*_L$ for all K, while the fit to the HRS observations gives $A^*_T/A^*_L = 12.0 \pm 0.6$. This indicates that the molecular orientation distribution for each K is a nearly pure transverse polar mode.

The molecular orientation distribution is constrained but not uniquely determined by the observations. Two alternative orientation distributions consistent with the experimental observations will be considered. The model distribution that has been previously considered[12] is randomly oriented spherical domains in which a small azimuthal orientation bias is imposed on the otherwise randomly oriented molecules in each domain. The transverse polar mode HRS intensity is $\propto a_1^2 K^2 r^8 \exp[-(Kr/2.6)^2]$ for such domains with radius r, where $a_1 = \langle \hat{\mu} \cdot \hat{\varphi} \rangle$ is the degree of ordering of the molecular dipole axis $\hat{\mu}$ around the azimuthal direction $\hat{\varphi}$ at each point in the domain. The K-independent value of A_T/A_0 observed for water could be obtained by filling the liquid with such domains which have size distribution $p(r) \propto r^{-7}$, molecular order $a_1 = 10^{-3}$ and minimum radius 23 nm. The spherical domains in this model are analogous to the radial polarized spherical domains induced by the electric field of individual ions in solution, which gives longitudinal polar mode HRS.[8,11] However, a mechanism that can produce azimuthally polarized

domains with the required size distribution is lacking, which argues against this model.

Acoustic phonons are known to be present in liquids, and an alternative proposal is that the observed long-range orientation correlations are produced by coupling molecular orientation to molecular displacement in phonons. Molecular alignment by molecular rotation-translation coupling is observed both in flow birefringence and the central dip in the depolarized light scattering spectrum for shear waves, and in ultrasonic induced birefringence for longitudinal waves.[13–17] Those experiments are all governed by the same dimensionless rotation-translation coupling parameter $0 \leq R_{RT} \leq 1$.[13] The experimentally observed value for this parameter is nearly temperature independent and falls in the range $R_{RT} = 0.4 \pm 0.2$ for a variety of liquids.[14–16] Molecular alignment measured in those experiments is closely related to molecular orientation probed by the present HRS experiment.

Only longitudinal phonons propagate in water for the wavevectors probed in these HRS experiments, so the HRS results suggest that longitudinal velocity gradients orient molecules in the liquid, analogous to the coupling in ultrasonic induced birefringence. The longitudinal phonon at each $\mathbf{K}$ is associated with a polar orientation mode, and the orientation distribution due to thermally excited acoustic phonons is a superposition of the associated polar orientation modes. The experimental observation $A^*_T/A^*_L = 12.0 \pm 0.6$ for water indicates that molecular orientation-translation coupling results in nearly pure transverse polar orientation modes. The orientation distribution of water molecules in the liquid, determined by superposition of transverse polar orientation modes, will be a transverse vector field.

Long-range orientation correlations are not limited to water. Previous HRS experiments provide evidence for polar collective modes in other liquids, with transverse polar modes most common, but with longitudinal polar modes also seen for some liquids.[4] Both transverse and longitudinal polar modes may be understood as the result of rotation-translation coupling in phonons for acentric, anisotropic molecules.

Orientation-translation coupling is found in a recent molecular dynamics simulation of water molecules in carbon nanotubes. The simulation finds that orienting the dipoles of the water molecules at about 35° to the nanotube axis results in net transport of water molecules in the direction of the dipoles, due to coupling between rotational and translational motions.[18] This result is suggestive, although it may not be directly applicable to the present case due to confinement effects.

Local structure and short-range correlations are measured in water using experimental techniques such as x-ray and neutron scattering[19] and nuclear magnetic resonance spectroscopy,[20] but these probes are insensitive to long-range orientation correlations. Vortex-like structures[21,22] or collective motions[23] have been found in several molecular dynamics (MD) simulations for water, similar in form to the azimuthal orientation correlations previously proposed[12] as an explanation of the HRS results. Dipolar orientation correlations at the nm scale have also been found using density functional theory[24] and MD simulations[25–27] for water. These results are not inconsistent with the long-range

orientation correlations in water observed by HRS, but are not conclusive since even the largest simulation box is <10 nm, much smaller that the length scale probed by the present HRS experiment.

In summary, the polarization and angle dependence of HRS measured for liquid water is not consistent with randomly oriented molecules or molecules with only short-range orientation correlations, but the HRS measurements are in good agreement with a liquid structure which is dominated by long-range transverse polar collective modes of molecular orientation. It is proposed that the long-range orientation correlations are the result of molecular rotation-translation coupling in acoustic phonons.

[1] D. Chandler, Acc. Chem. Res. **7**, 246 (1974).
[2] P. M. Chaikin and T. C. Lubensky, *Principles of Condensed Matter Physics* (Cambridge University Press, Cambridge, UK, 1995).
[3] J.-L. Barrat and J.-P. Hansen, *Basic Concepts for Simple and Complex Liquids* (Cambridge University Press, Cambridge, UK, 2003).
[4] D. P. Shelton, J. Chem. Phys. **136**, 044503 (2012).
[5] P. D. Maker, Phys. Rev. A **1**, 923 (1970).
[6] R. Bersohn, Y. H. Pao, and H. L. Frisch, J. Chem. Phys. **45**, 3184 (1966).
[7] D. P. Shelton, Rev. Sci. Instrum. **82**, 113103 (2011).
[8] D. P. Shelton, J. Chem. Phys. **138**, 054502 (2013).
[9] D. P. Shelton, J. Opt. Soc. Am. B **17**, 2032 (2000).
[10] D. P. Shelton, J. Chem. Phys. **132**, 154506 (2010).
[11] D. P. Shelton, J. Chem. Phys. **130**, 114501 (2009).
[12] D. P. Shelton, J. Chem. Phys. **138**, 154502 (2013).
[13] R. Lipeles and D. Kivelson, J. Chem. Phys. **67**, 4564 (1977).
[14] W. Lempert and C. H. Wang, J. Chem. Phys. **72**, 3490 (1980).
[15] D. Kivelson and P. A. Madden, Ann. Rev. Phys. Chem. **31**, 523 (1980).
[16] T. Shibata, T. Matsuoka, K. Yasuda, S. Koda, and H. Nomura, J. Chem. Phys. **109**, 2038 (1998).
[17] T. Matsuoka, K. Yasuda, S. Koda, and H. Nomura, J. Chem. Phys. **111**, 1580 (1999).
[18] S. Joseph and N. R. Aluru, Phys. Rev. Lett. **101**, 064502 (2008).
[19] G. N. I. Clark, C. D. Cappa, J. D. Smith, R. J. Saykally, and T. Head-Gordon, Mol. Phys. **108**, 1415 (2010).
[20] F. Mallamace, C. Corsaro, D. Mallamace, S. Vasi, C. Vasi, and H. E. Stanley, J. Chem. Phys. **141**, 18C504 (2014).
[21] J. Higo, M. Sasai, H. Shirai, H. Nakamura, and T. Kugimiya, Proc. Natl. Acad. Sci. U.S.A. **98**, 5961 (2001).
[22] A. N. Dickey and M. J. Stevens, Phys. Rev. E **86**, 051601 (2012).
[23] V. P. Voloshin, G. G. Malenkov, and Y. I. Naberukhin, J. Struct. Chem. **54**, S233 (2013).
[24] Y. Liu and J. Wu, J. Chem. Phys. **139**, 041103 (2013).
[25] P. Kumar, G. Franzese, S. V. Buldyrev, and H. E. Stanley, Phys. Rev. E **73**, 041505 (2006).
[26] D. C. Elton and M.-V. Fernandez-Serra, J. Chem. Phys. **140**, 124504 (2014).
[27] C. Zhang and G. Galli, J. Chem. Phys. **141**, 084504 (2014).